Polyhedron 102 (2015) 130–136

Contents lists available at ScienceDirect

Polyhedron

journal homepage: www.elsevier.com/locate/poly

Neodymium coordination polymers with propionate, succinate and mixed succinate–oxalate ligands: Synthesis, structures and spectroscopic characterization

Nicholas Scales [a], Yingjie Zhang [a,*], Mohan Bhadbhade [b], Inna Karatchevtseva [a], Linggen Kong [a], Gregory R. Lumpkin [a], Feng Li [c]

[a] Australian Nuclear Science and Technology Organisation, Locked Bag 2001, Kirrawee DC, NSW 2232, Australia
[b] Mark Wainwright Analytical Centre, University of New South Wales, Kensington, NSW 2052, Australia
[c] School of Science and Health, University of Western Sydney, Locked Bag 1797, Penrith, NSW 2751, Australia

A R T I C L E I N F O

Article history:
Received 27 May 2015
Accepted 28 July 2015
Available online 7 August 2015

Keywords:
Neodymium
Coordination polymer
Propionate
Succinate
Oxalate

ABSTRACT

Three neodymium (Nd) coordination polymers with propionate, succinate and mixed succinate–oxalate ligands have been synthesized and structurally characterized. $Nd_2(C_3H_5O_2)_6(H_2O)_3{\cdot}3H_2O$ (**1**) has a 1D polymeric structure built with both ninefold and ten-fold coordinated neodymium polyhedra linked through μ_2-bridging propionate ligands. $Nd_2(C_4H_4O_4)_3(H_2O)_2$ (**2**) has a 3D polymeric structure constructed with two distinct ninefold coordinated neodymium polyhedra linked through three types of succinate ligands, two in μ_4- and one in μ_3-coordination modes. $Nd_2(C_4H_4O_4)_2(C_2O_4)(H_2O)_4{\cdot}3H_2O$ (**3**) is built with two types of ten-fold coordinated neodymium polyhedra linked through μ_4-succinate ligands into 2D undulating layers which are further connected through μ_2-oxalate ligands forming a 3D network with channels. Their vibrational modes and thermal stabilities have been further investigated.

1. Introduction

Lanthanoid metal–organic frameworks (MOFs) and coordination polymers (CPs) have attracted recent interest due to their potential industrial applications, e.g. gas adsorption, non-linear-optical (NLO) materials, heterogeneous catalysis, magnetism, luminescence, molecular sensing, separation and molecular recognition, as well as their structural diversity and interesting topological networks [1–2]. In general, bridging organic ligands are required to bind metal ions in various coordination modes in order to build such MOFs and CPs. Among the various bridging ligands, mono-/di-carboxylic acids have been extensively studied [3–4].

More recently, neodymium (Nd) organic complexes and coordination polymers have shown interesting catalysis effect on some organic polymerisation reactions, which has subjected to further investigations [5]. This contribution deals with Nd coordination polymers with propionate and succinate ligands. A neodymium propionate complex with a one-dimensional (1D) structure has previously been reported [6], see Structure description and discussion section. Although the synthetic procedure was not readily available, it is anticipated that the complex would be prepared by the aqueous reaction of neodymium(III) ion with a deprotonated propionate salt, similar to the method for the preparation of other neodymium butyrate complexes [7]. Apart from the deposited crystal structure data, no other spectroscopic characterization on this complex was available. Therefore, it is of interest to further examine the structural diversity of neodymium–propionate system through a slightly different reaction route. In addition, succinic and oxalic acids are very common dicarboxylate ligands which have been widely used as effective linkers to build CPs and MOFs [1]. Several neodymium complexes with succinate or succinate and oxalate have been reported and 3D frameworks are dominating [8–9]. As both succinate and oxalate are very flexible, the structural diversity is far from limited and deserves further effort. Herein we report the synthesis, spectroscopic studies and crystal structures of three neodymium coordination polymers: $Nd_2(C_3H_5O_2)_6(H_2O)_3{\cdot}3H_2O$ (**1**) with propionate, $Nd_2(C_4H_4O_4)_3(H_2O)_2$ (**2**) with succinate and $Nd_2(C_4H_4O_4)_2(C_2O_4)(H_2O)_4{\cdot}3H_2O$ (**3**) with mixed succinate–oxalate ligands.

---

* Corresponding author.
E-mail address: yzx@ansto.gov.au (Y. Zhang).

http://dx.doi.org/10.1016/j.poly.2015.07.065
0277-5387/

Table 1
Crystal data and refinement details for **1–3**.

Complex	**1**	**2**	**3**
Formula	$C_{18}H_{41}O_{18}Nd_2$	$C_{12}H_{12}O_{14}Nd_2$	$C_{10}H_{14}O_{19}Nd_2$
Formula weight	833.99	668.70	726.69
Crystal system	monoclinic	triclinic	monoclinic
Space group	$P2_1/c$	$P\bar{1}$	$C2/c$
a (Å)	10.2631(5)	7.8110(16)	9.6827(10)
b (Å)	15.0716(7)	8.1000(16)	27.686(3)
c (Å)	20.5876(9)	14.188(3)	9.1050(7)
α (°)	90	96.75(3)	90
β (°)	102.736(3)	96.67(3)	121.794(3)
γ (°)	90	103.63(3)	90
V (Å^3)	3106.2(3)	856.6(3)	2074.5(3)
Z	4	2	4
μ (mm^{-1})	3.376	6.070	5.040
D_{calc} (g cm^{-3})	1.783	2.592	2.327
Min./Max. θ (°)	2.437/24.999	1.46/32.44	1.471/24.997
Goodness-of-fit (GOF) on F^2	1.013	1.035	1.455
Final R_1 [a] $[I > 2\sigma(I)]$	0.0414	0.0419	0.0524
Final wR_2 [b] $[I > 2\sigma(I)]$	0.0874	0.1057	0.1325

[a] $R_1 = \Sigma||F_o| - |F_c||/|F_o|$.
[b] $wR_2 = \{\Sigma[w(F_o^2 - F_c^2)^2]/\Sigma[w(F_o^2)^2]\}^{1/2}$.

2. Results and discussion

2.1. Structure description and discussion

The crystallographic data and refinement details for complexes **1**–**3** are shown in Table 1 and the Nd-O bond lengths in **1**–**3** are summarized in Table 2. $Nd_2(C_3H_5O_2)_6(H_2O)_3 \cdot 3H_2O$ (**1**): The structure of **1** is constructed by two crystallographically distinct neodymium polyhedra linked through propionate ligands forming a 1D undulating polymer (Fig. 1). Nd1 has a ten-fold coordination polyhedron with four chelating ligands [Nd1–O bonds from 2.484(4) Å to 2.655(4) Å] and two bridging carboxylate O atoms [Nd1–O bonds from 2.465(4) Å to 2.495(4) Å] (Fig. 1a and b). Nd2 has a ninefold coordination polyhedron with two chelating ligands [Nd2–O bonds from 2.493(4) Å to 2.601(4) Å], two bridging carboxylate O atoms [Nd2–O distances from 2.441(4) Å to 2.445(4) Å] and three water molecules [Nd2–O_{H2O} bonds from 2.447(5) Å to 2.490(4) Å]. The distance between Nd1 and Nd2 is ~4.310 Å. Pairs of Nd1 and Nd2 polyhedra are linked through μ_2-(η^2:η^1) bridging ligands forming 1D undulated polymeric chains along the crystallographic b-axis (Fig. 1c and d). Nd1 has a polyhedron close to a bicapped square antiprism and Nd2 has a polyhedron close to a capped square antiprism. The calculated possible intra-molecule hydrogen bonds are summarized in Table 3. Both coordinated and lattice water molecules are involved in extensive hydrogen bonding with carboxylate oxygen atoms leading the 1D polymer into three dimensions.

Another neodymium propionate complex, **T**, has previously been reported [6]. It is a 1D polymeric structure constructed by both μ_2-(η^2:η^1) and μ_2-(η^1:η^1) bridging propionate ligands. It is of interest to examine the similarities and differences between **1** and **T**. The connection topologies of both complexes are shown in Fig. 2 and their Nd coordination environments together with connection features are summarized in Table 4. Both **1** and **T** have 1D polymeric structures built with neodymium(III) ion and propionate ligand. However, there are several differences between them. Firstly, they crystallize in different space groups with different cell parameters. Secondly, they have different neodymium coordination environments: two ninefold coordinated neodymium centres in **T**; a ninefold and a ten-fold coordinated neodymium centres in **1**. Thirdly, propionate ligands have different coordination modes: chelating and μ_2-(η^2:η^1) bridging in **1**; monodentate, μ_2-(η^1:η^1) and μ_2-(η^2:η^1) bridging in **T**. Fourthly, **1** has relatively longer average Nd–O bond length and wider Nd–Nd–Nd angle suggesting a more flat conformation compared to **T**. Finally, the connection topologies are different: repeat Nd1–Nd2 in **1** and repeat Nd1–Nd1–Nd2–Nd2 in **T**.

2.2. $Nd_2(C_4H_4O_4)_3(H_2O)_2$ (2)

The structure of **2** is constructed with two crystallographically distinct ninefold coordinated Nd polyhedra (Fig. 3a and b). Both Nd1A and Nd1B have similar coordination environments: one water molecule [2.508(4) Å for Nd1A–O5A and 2.471(4) Å Nd1B–O5B], two μ_2-(η^1:η^1) [O2C and O2B with mean Nd1A–O bond length of 2.464(4) Å; O1C and O1B with mean Nd1B–O bond length of 2.423(4) Å], two μ_2-(η^1:η^2) [O3A and O4B with mean Nd1A–O bond length of 2.455(4) Å; O2A and O4C with mean Nd1B–O bond length of 2.460(4) Å] and four μ_2-(η^2:η^1) [O1A, O2A, O3C and O4C with mean Nd1A–O bond length of 2.528(4) Å; O3A, O4A, O3B and O4B with mean Nd1B–O bond length of 2.572(3) Å] carboxylate oxygen atoms. The distance between Nd1A and Nd1B is about 4.114(1) Å. Pairs of Nd1A and Nd1B are linked together through two types of μ_2-carboxylate arms forming 1D polymeric chains along the a-axis (Fig. 3c). The 1D chains formed by edge-sharing between Nd1A and Nd1B are further linked by succinate ligands through two types of μ_4- coordination modes [(η^1:η^1:η^1:η^2) and (η^1:η^2:η^1:η^2)] forming a 3D pillared framework (Fig. 3d). Only non-classical hydrogen bonds exist involving some carboxylate oxygen atoms and CH_2– groups (see Table 3). Three structures of neodymium succinate complexes have been reported [8]. Two of

Table 2
Selected bond lengths (Å) for complexes **1–3**.

*Complex **1***							
Nd1–O1A	2.528(4)	Nd1–O1B	2.546(4)	Nd1–O1C	2.482(4)	Nd1–O1D	2.495(4)
Nd1–O1E	2.465(4)	Nd1–O1F	2.655(4)	Nd1–O2A	2.553(4)	Nd1–O2B	2.607(4)
Nd1–O2C	2.697(4)	Nd1–O2F	2.488(4)	Nd2–O1F#	2.445(4)	Nd2–O1D#	2.589(4)
Nd2–O1E#	2.601(4)	Nd2–O2D	2.575(4)	Nd2–O2E	2.493(4)	Nd2–O1W	2.447(5)
Nd2–O2W	2.490(4)	Nd2–O3W	2.453(4)	Nd2–O2C#	2.697(4)		
*Complex **2***							
Nd1A–O1A	2.517(4)	Nd1A–O2A	2.533(3)	Nd1A–O3A	2.480(4)	Nd1A–O5A	2.508(4)
Nd1A–O2B	2.517(4)	Nd1A–O4B	2.430(3)	Nd1A–O2C	2.410(4)	Nd1A–O3C	2.520(4)
Nd1A–O4C	2.548(3)	Nd1B–O2A#	2.467(4)	Nd1B–O3A#	2.578(3)	Nd1B–O4A	2.518(4)
Nd1B–O1B	2.406(3)	Nd1B–O3B	2.510(4)	Nd1B–O4B#	2.595(3)	Nd1B–O5B	2.471(4)
Nd1B–O1C	2.436(4)	Nd1B–O4C#	2.453(3)				
*Complex **3***							
Nd1A–O1A	2.43(2)	Nd1A–O2A	2.62(3)	Nd1A–O3A	2.54(2)	Nd1A–O4A	2.55(2)
Nd1A–O5A	2.438(19)	Nd1A–O6A	2.53(2)	Nd1A–O1A#	2.86(3)	Nd1A–O5A#	2.85(3)
Nd1A–O1	2.465(18)	Nd1A–O2	2.516(19)	Nd1B–O1B	2.44(2)	Nd1B–O2B	2.56(3)
Nd1B–O3B	2.61(3)	Nd1B–O4B	2.42(2)	Nd1B–O5B	2.50(2)	Nd1B–O6B	2.55(2)
Nd1B–O1B#	2.86(2)	Nd1B–O4B#	2.90(2)	Nd1B–O3	2.463(18)	Nd1B–O4	2.52(2)

them are in higher symmetry space groups, e.g. monoclinic and orthorhombic [8a,b] and only one is in triclinic space group which has a very similar structure [8c].

2.3. $Nd_2(C_4H_4O_4)_2(C_2O_4)(H_2O)_4·3H_2O$ (**3**)

The structure of **3** is built up with two types of ten-fold coordinated neodymium polyhedra (Fig. 4a and b). Both Nd1A and Nd1B have similar coordination environments: two water molecules [O3A and O4A with mean Nd1A–O bond length of 2.54(2) Å; O5B and O6B with mean Nd1B–O bond length of 2.53(2) Å], two μ_2-oxalato [O1 and O2 with mean Nd1A–O bond length of 2.490(18) Å; O3 and O4 with mean Nd1B–O bond length of 2.491(18) Å], four μ_2-(η^2:η^1) [O1A, O2A, O5A and O6A with mean Nd1A–O bond length of 2.51(3) Å; O1B, O2B, O3B and O4B with mean Nd1B–O bond length of 2.51(3) Å] and two μ_2-(η^1:η^2) [O5A# and O1A# with mean Nd1A–O bond length of 2.86(2) Å; O1B# and O4B# with mean Nd1B–O bond length of 2.88(2) Å] carboxylate oxygen atoms. Neodymium polyhedra are connected through corner-sharing O atoms forming 1D polymeric chains (Fig. 4c) which are further linked through μ_4-(η^1:η^2:η^1:η^2) succinate ligands into 2D pillared layers (Fig. 4d). Alternating Nd1A and rotated 90° Nd1B layers are linked through μ_2-bridging oxalate ligands forming a 3D framework structure (Fig. 4e). Both coordinated and lattice water molecules sitting inside the channels along the crystallographic *a*-axis are involved in hydrogen bonding (see Table 3). Two neodymium succinate–oxalate mixed ligand complexes were previously reported [9]. One is in triclinic space group with a smaller unit cell and has a slightly different 3D structure [9a]. The other one has a similar 3D structure as complex **3** but in orthorhombic space group with a relatively larger unit cell [9b].

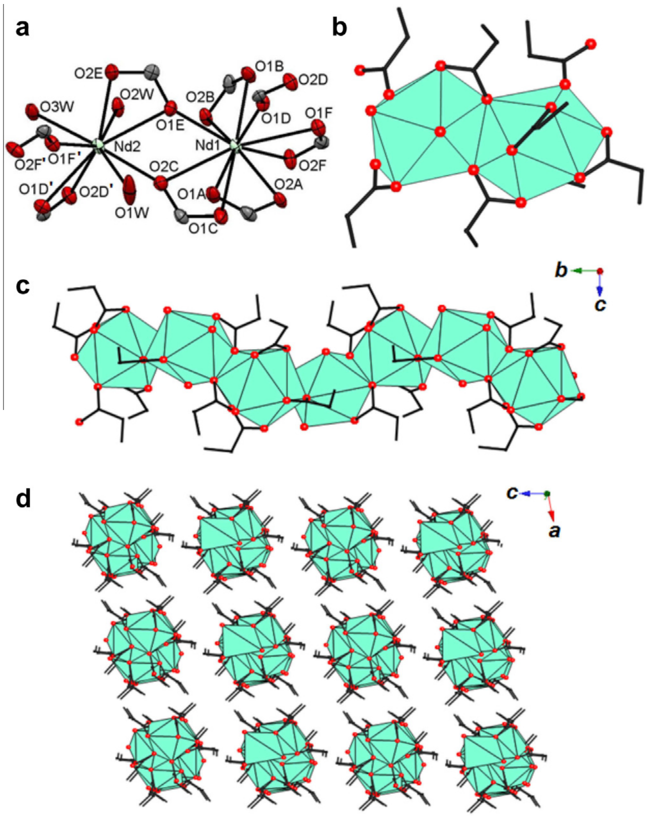

Fig. 1. Structure of **1**: Ellipsoid (a) and polyhedral (b) views of the two neodymium coordination polyhedra [ten-fold (Nd1); ninefold (Nd2)], which are linked through μ_2-bridging ligands forming a 1D undulating polymer (c) and a polyhedral packing view (d) along the crystallographic b-axis.

Table 3
Calculated possible hydrogen bonds for complexes **1**–**3**.

Donor	Acceptor	H. . .A	D. . .A	D–H. . .A
*Complex **1***				
O1W	O1B	1.80	2.673(7)	179
O2W	O2B	2.01	2.806(6)	152
O3W	O2A	1.88	2.748(6)	172
O4W	O2D	1.98	2.845(6)	175
O5W	O2B	1.90	2.764(6)	169
O6W	O1C	2.43	3.082(6)	132
O6W	O2F	2.39	3.195(6)	154
*Complex **2***				
C2A	O3B	2.52	3.277(6)	135
C3A	O3C	2.58	3.338(7)	135
C2C	O3C	2.47	2.816(7)	101
C3C	O1A	2.34	3.108(7)	135
*Complex **3***				
O3A	O2W	2.06	2.81(3)	142
O3A	O1W	2.21	2.90(4)	135
O4A	O3A	2.60	2.96(3)	105
O4A	O4W	1.97	2.79(4)	150
O4A	O3W	2.35	3.08(6)	138
O5B	O4W	2.33	3.06(6)	142
O5B	O4	1.88	2.76(3)	178

The typical coordination modes of the two ligands (propionate and succinate) which have been mentioned in this study are shown in Fig. 5. For propionate, three types of coordination modes, chelating (Fig. 5a), μ_2-(η^1:η^1) (Fig. 5b) and μ_2-(η^2:η^1) (Fig. 5c) have been observed before [6]. However, only chelating and μ_2-(η^2:η^1) have been found in complex **1**. Although there are many possible coordination modes for succinate ligand ranging from μ_2- to μ_4-, only two types of μ_4-bridging modes (Fig. 5d, e) have been observed in complexes **2** and **3**. As for oxalate, only the most common μ_2-bridging mode has been observed in complex **3**.

It is of interest to examine and compare mean Nd–O bond lengths of **1**–**3** with the statistic value obtained by Shannon [10] although only relevant value with coordination number (CN) of nine is available. Based on the CN of nine, the mean Nd–O bond length would be 2.583 Å which is slightly longer than the mean

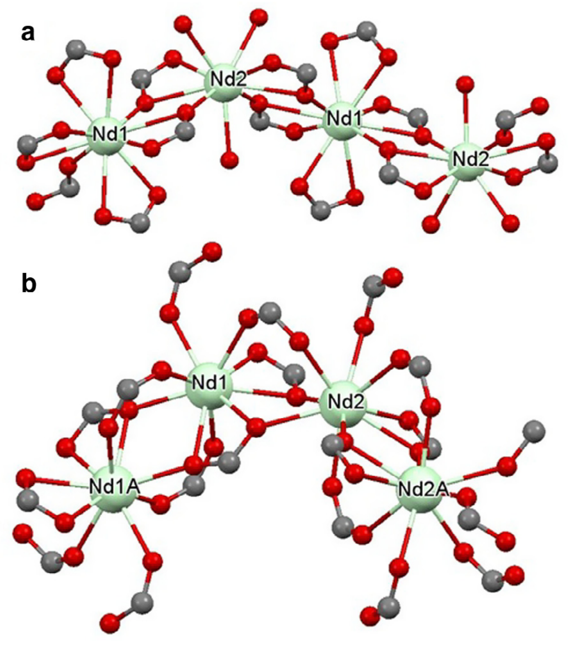

Fig. 2. Neodymium coordination environments and connection topologies of **1** (a) and a complex **T** [6] (b).

Table 4
Neodymium coordination environments and connection topologies for **1** and **T** [6].

Coordination/Complex	**1**		**T**	
	Nd1	Nd2	Nd1	Nd2
Coordination Number	10	9	9	9
Nd–O (COO) distance (Å)	2.465(4)–2.655(4)	2.441(4)–2.601(4)	2.395(2)–2.563(2)	2.379(2)–2.567(2)
Nd–O (H_2O) distance (Å)		2.447(5)–2.490(4)		
Average Nd–O (Å)	2.529(4)		2.494(2)	
Nd–Nd (Å)	4.310(4)		4.032(2)–4.139(2)	
Nd–Nd–Nd angle (°)	139.15(4); 140.55(4)		118.42(2); 142.30(2)	
Connection topology	Nd1:Nd2		Nd1:Nd1:Nd2:Nd2	

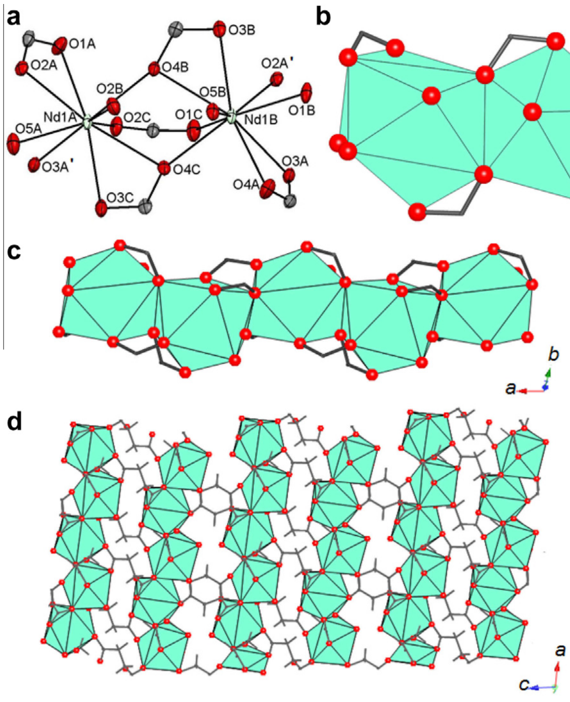

Fig. 3. Structure of **2**: Ellipsoid (a) and polyhedral (b) views of the two ninefold coordinated neodymium polyhedra, pairs of Nd1A and Nd1B polyhedra linked together through edge-sharing forming a 1D polymeric chain (c) and a polyhedral view (d) along the *b*-axis showing 1D chains are linked through μ_4-bridging ligands forming a 3D polymeric structure.

Nd–O bond values determined in this study, 2.544(4) Å for **1**, 2.494(5) Å for **2** and 2.58(3) Å for **3**.

2.4. Thermogravimetric and differential thermal analysis (TG/DTA)

The thermal stabilities of **1** and **3** have been examined. On the differential thermal analysis (DTA) curve of complex **1** (Fig. S2), there is an endotherm at ~97 °C associated with a weight loss of ~13.0% corresponding to the complete loss of six water molecules (calc. 12.9%). A small endotherm at 325 °C and a large exotherm at 375 °C correspond to the decomposition of propionate ligands. The last feature is a small endotherm at 650 °C with around 5% of weight loss corresponding to the phase change from $Nd_2(CO_3)_3$ to $(NdO)_2CO_3$, and to the final product, Nd_2O_3 [11] as the residue ~41.0% (calc. 40.3%). On the DTA curve of complex **3** (Fig. S2), there are two endotherms at ~200 °C and 345 °C associated with a total weight loss of ~16.8% corresponding to the loss of both lattice and coordinated water molecules (cacl. 17.1%). A large exotherm at ~460 °C together with two small exotherms at ~550 °C and 670 °C correspond to the decomposition of organic ligands and the formation of the final product, Nd_2O_3, with the residue ~45.5% (calc. 45.8%).

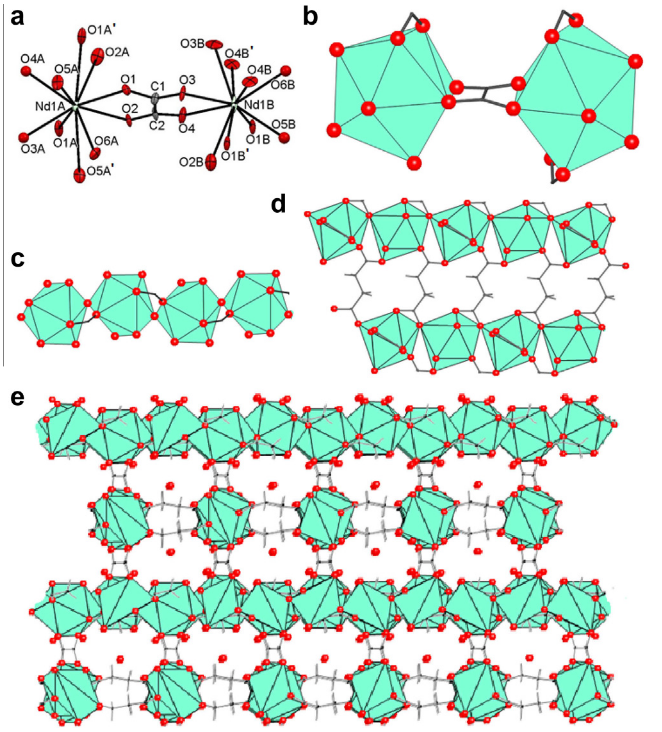

Fig. 4. Structure of **3**: Ellipsoid (a) and polyhedral (b) views of the two ten-fold coordinated neodymium polyhedra, Nd1A or Nd1B polyhedra connected through corner-sharing forming 1D chains (c) which are linked through succinate ligands into 2D pillared sheets (d), and Nd1A sheets and rotated 90° Nd1B sheets linked through μ_2-bridging oxalate ligands forming a 3D polymeric structure (e).

2.5. Raman spectroscopy

Raman spectra of **1**–**3** are shown in Fig. 6. The Raman assignments are based on some relevant literature data [12] and detailed assignments are summarized in Table S1.

The absence of Raman peak at 1690 cm^{-1} due to carbonyl (C=O) stretching in complex **1** indicates that all carboxyl groups are completely deprotonated, and as such Raman bands located at 1555 and 1422 cm^{-1} have been assigned to asymmetric and symmetric stretching modes, respectively, of the carboxylate groups coordinated to neodymium ions. The strong Raman band at 1451 cm^{-1} is due to the asymmetric bending vibration δ_{as} (CH_3), with a shoulder at lower frequency side due to the δ (CH_2) deformation vibrations. The symmetric bending vibration δ_s (CH_3) is located at 1377 cm^{-1}. The bands at 1301 and 1250 cm^{-1} can be assigned to the wagging and twisting vibrations δ (CH_2), respectively, while the δ (CH_2) rocking is observed at 740 cm^{-1}. Multiple strong bands in the region of 1077–899 cm^{-1} are due to the skeletal ν(C–C–C) and ν(C–C) stretching vibrations. The C–C deformation band is located at 513 cm^{-1}. The bands at 815 and

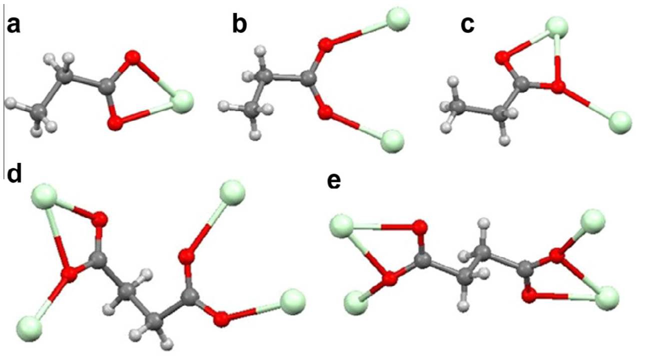

Fig. 5. Observed coordination modes of propionate [chelating (a), μ_2-(η^1:η^1) (b) and μ_2-(η^2:η^1) (c)] and succinate [μ_4-(η^1:η^1:η^2:η^1) (d) and μ_4-(η^2:η^1:η^2:η^1)] ligands.

679 cm^{-1} are due to the δ (OCO) in-plane and out-of-plane deformation modes. The broad band at around 643 cm^{-1} is due to the vibrational deformation modes of coordinated water molecules. The ν(M–O) stretching vibration is located at 311 cm^{-1} and bands below 300 cm^{-1} are due to the δ (C–O–M) deformation, torsional vibration of δ (CH_3), as well as lattice modes.

The Raman spectra of complexes **2** and **3** are very similar due to the presence of same succinate ligand with the most noteworthy observation of a very strong band at around 1462 cm^{-1}, with the intensity stronger in **2** compared to **3**. This strong band is due to the C···O species where the electron density is distributed evenly [13], suggesting tetradentate chelating ligand linking two metal centres. Other Raman bands and assignments are similar to those for **1** (see Table S1).

3. Conclusions

The dissolution of freshly precipitated $Nd(OH)_3$ with propionic acid leads to the formation of a new neodymium propionate complex. $Nd_2(C_3H_5O_2)_6(H_2O)_3{\cdot}3H_2O$ (**1**) has a 1D polymeric structure built with both ninefold and ten-fold coordinated neodymium polyhedra linked through μ_2-bridging propionate ligands. Two neodymium coordination polymers with succinate or mixed succinate–oxalate ligands have been synthesized under hydrothermal conditions. $Nd_2(C_4H_4O_4)_3$ $(H_2O)_2$ (**2**) has a 3D polymeric structure constructed with two distinct ninefold coordinated Nd polyhedra linked through three types of succinate ligands, two with μ_4- and one with μ_3-bridging coordination modes. $Nd_2(C_4H_4O_4)_2(C_2O_4)(H_2O)_4{\cdot}3H_2O$ (**3**) has a 3D network structure built with two types of ten-fold coordinated neodymium polyhedra linked through μ_4-succinate ligands first into 2D undulating layers which are further connected through μ_2-oxalate ligands. Complex **3** has various channels viewed at different directions. Thermal analysis confirmed that both **1** and **3** lost lattice and coordinated water molecules first, followed by the decomposition of organic ligands to form the final product, Nd_2O_3. Raman characterization confirmed the presence of propionate or succinate ligands in **1**–**3**.

4. Experimental

4.1. Synthesis

4.1.1. $Nd_2(C_3H_5O_2)_6(H_2O)_3{\cdot}3H_2O$ (*1*)

Complex **1** was synthesized at room temperature by dissolving freshly prepared $Nd(OH)_3$ with propionic acid. Neodymium nitrate hexahydrate (0.44 g, 1.0 mmol) was dissolved in 5.0 mL deionized (DI) water. To the above solution, 1.0 mL concentrated ammonia

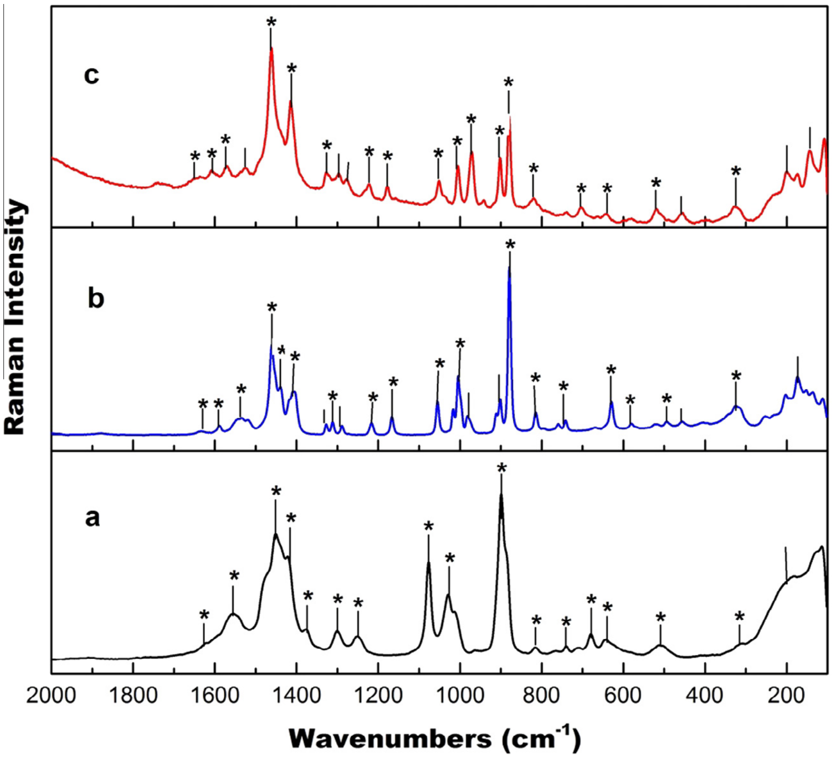

Fig. 6. Raman spectra of **1** (a), **2** (b) and **3** (c) in 2000–100 cm^{-1} region (*represents assigned bands).

solution was added to precipitate neodymium(III) ions as $Nd(OH)_3$. The precipitation was washed with DI water for three times to remove the excess ammonia and then was dissolved in 1.0 mL of concentrated propionic acid and 5.0 mL of DI water. Colorless crystalline product was formed in three weeks after slow evaporation with 84% yield. Formula: $C_{18}H_{42}O_{18}Nd_2$ (FW = 835.0), *Anal.* Calc. C, 25.89; H, 5.05. Found: C, 25.82; H, 5.11%.

4.1.2. $Nd_2(C_4H_4O_4)_3(H_2O)_2$ (**2**) and $Nd_2(C_4H_4O_4)_2(C_2O_4)(H_2O)_4 \cdot 3H_2O$ (**3**)

Neodymium nitrate hexahydrate (0.44 g, 1.0 mmol), $(NH_4)_2C_2O_4 \cdot H_2O$ (0.07 g, 0.5 mmol) and succinic acid (0.12 g, 1.0 mmol) were added to a 120 mL Teflon container with 10.0 mL of DI water. The Teflon container was then sealed in a stainless steel pressure Par vessel and left in a 180 °C oven for 48 h. Two types of light pink crystalline products were obtained after slow cooling (<10 °C/h) to room temperature. Complex **2** was crystallized as fine needles with estimated yield of less than 30%. Complex **3** was crystallized as poor quality large crystals with approximately 35% yield. Recrystallization of **3** in aqueous solution was attempted. However, no obvious improvement of crystal quality could be achieved.

As **2** and **3** were formed in the same reaction mixture, small amounts of **3** were manually separated for further characterizations whilst the fine needle of complex **2** was only characterized by single crystal X-ray diffraction. The powder X-ray diffraction (PXRD) patterns of **1** and **3** (Fig. S1) obtained from the bulk materials match the patterns generated from the single crystal data, suggesting that **1** and **3** in pure phase form have been obtained.

4.2. Characterization

4.2.1. Single crystal X-ray diffraction

The single-crystal data for **1** and **3** were collected on a Bruker kappa-II CCD diffractometer at 150 K by using graphite-monochromated Mo Kα radiation (λ = 0.71073 Å). Symmetry related absorption corrections using the program SADABS were applied and the data were corrected for Lorentz and polarisation effects using Bruker APEX2 software [14]. Single-crystal X-ray data for **2** were collected at 100(2) K on MX1 beamline at the Australian Synchrotron with Silicon Double Crystal radiation (λ = 0.71080 Å) using BlueIce software [15]. Lorentz and polarisation effects were corrected and cell refinements and data reductions were carried out using XDS software [16]. The structures were solved by direct methods and the full-matrix least-squares refinements were carried out using SHELX [17] via Olex^2 interface [18]. Structural refinements were straightforward for **1** and **2** with all non-hydrogen atoms located from the electron density maps and refined anisotropically except for the low occupancy water molecules in **2** which were refined isotropically. The one circle goniometer at the Australian Synchrotron limits the data collection. Therefore, the data completeness is low for **2**. The refinement of **3** was difficult due to the poor quality data collected as a result of poor single crystal nature and ineffective absorption correction treatment. Consequently, some restraints are necessary and all water molecules have been refined isotropically. Potential hydrogen bonds were calculated for **1**–**3** using PLATON [19].

4.2.2. Elemental analyses

Elemental analyses were carried out using a Perkin–Elmer 2400 CHN elemental analyzer.

4.2.3. Powder X-ray diffraction (PXRD)

PXRD data were collected on a X'Pert Pro with Cu K*a* radiation, in the range 5° < 2θ < 60°, with a step size of 0.02° (2θ) and an acquisition time of 2 s per step.

4.2.4. Raman spectroscopy

Raman spectra were collected using a Renishaw inVia Raman spectrometer equipped with a monochromator, a filter system and a Peltier-cooled Charge-Coupled Device (CCD). It was excited by an argon ion laser (514.5 nm) and collected in the range of 2000–100 cm^{-1} with a spectral resolution of ~1.7 cm^{-1}. Spectra were calibrated using the 520.5 cm^{-1} line of a silicon wafer.

4.2.5. Thermogravimetric and differential thermal analysis (TG/DTA)

Thermogravimetric and differential thermal analysis (TG/DTA) were made on a SEIKO 6300 Thermal Analyzer from room temperature to 1000 °C with a heating rate of 10 °C min^{-1} and an air flow rate of 300 cm^3 min^{-1}.

Acknowledgements

The single crystal data for complex **2** were collected on the MX1 beamline at the Australian Synchrotron, Victoria, Australia.

Appendix A. Supplementary data

CCDC 1402821 (**1**), 1402822 (**2**) and 1402823 (**3**) contains the supplementary crystallographic data for **1**–**3**. These data can be obtained free of charge via http://www.ccdc.cam.ac.uk/conts/retrieving.html, or from the Cambridge Crystallographic Data Centre, 12 Union Road, Cambridge CB2 1EZ, UK; fax: (+44) 1223 336 033; or e-mail: deposit@ccdc.cam.ac.uk. Supplementary data associated with this article can be found, in the online version, at http://dx.doi.org/10.1016/j.poly.2015.07.065.

References

[1] (a) O.M. Yaghi, M. O'Keeffe, N.W. Ockwig, H.K. Chae, M. Eddaoudi, J. Kim, Nature 423 (2003) 705;
(b) C.-H. Huang, Rare Earth Coordination Chemistry: Fundamentals and Applications, John Wiley & Sons (Asia) Pte Ltd, 2010;
(c) S. Kitagawa, R. Kitaura, S.-I. Noro, Angew. Chem., Int. Ed. 43 (2004) 2334;
(d) L. Ma, C. Abney, W. Lin, Chem. Soc. Rev. 38 (2009) 1248;
(e) L.J. Murray, M. Dinca, J.R. Long, Chem. Soc. Rev. 38 (2009) 1294;
(f) J.Y. Lee, O.K. Farha, J. Roberts, K.A. Scheidt, S.T. Nguyen, J.T. Hupp, Chem. Soc. Rev. 38 (2009) 1450;
(g) J.J. Perry IV, J.A. Perman, M.J. Zaworotko, Chem. Soc. Rev. 38 (2009) 1400;
(h) A.K. Cheetham, C.N.R. Rao, R.K. Feller, Chem. Commun. (2006) 4780;
(i) T.R. Cook, Y.-R. Zheng, P.J. Stang, Chem. Rev. 113 (2013) 734.

[2] (a) J.-R. Li, R.J. Kuppler, H.-C. Zhou, Chem. Soc. Rev. 38 (2009) 1477;
(b) A.U. Czaja, N. Trukhan, U. Muller, Chem. Soc. Rev. 38 (2009) 1284;
(c) K. Binnemans, Chem. Rev. 109 (2009) 4283;
(d) M.D. Allendorf, C.A. Bauer, R.K. Bhakta, R.J.T. Houk, Chem. Soc. Rev. 38 (2009) 1203.

[3] (a) Z. Majeed, G.E. Kostakis, Y. Lan, A.K. Powell, Dalton Trans. 40 (45) (2011) 12210;
(b) Y. Luo, K. Bernot, G. Calvez, S. Freslon, C. Daiguebonne, O. Guillou, N. Kerbellec, T. Roisnel, CrystEngComm 15 (2013) 1882;
(c) Y. Zhang, M. Bhadbhade, N. Scales, I. Karatchevtseva, J.R. Price, K. Lu, G.R. Lumpkin, J. Solid State Chem. 219 (2014) 1;
(d) C.-J. Li, W. Li, Z.-S. Meng, M.-X. Peng, M.-M. Yang, M.-L. Tong, Aust. J. Chem. 62 (2009) 1607;
(e) Y.-C. Chen, F.-S. Guo, Y.-Z. Zheng, J.-L. Liu, J.-D. Leng, R. Tarasenko, M. Orendáč, J. Prokleška, V. Sechovský, M.-L. Tong, Chem. Eur. J. 19 (2013) 13504.

[4] (a) Y.-Z. Zheng, M. Evangelisti, R.E.P. Winpenny, Angew. Chem., Int. Ed. 50 (2011) 3692;
(b) A.P. Milanov, R.W. Seidel, D. Barreca, A. Gasparotto, M. Winter, J. Feydt, S. Irsen, H.-W. Becker, A. Devi, Dalton Trans. 40 (2011) 62;
(c) X.-J. Zhang, Y.-H. Xing, Z. Sun, J. Han, Y.-H. Zhang, M.-F. Ge, S.-Y. Niu, Cryst. Growth Des. 7 (2007) 2041;
(d) C.-G. Wang, Y.-H. Xing, Z.-P. Li, J. Li, X.-Q. Zeng, M.-F. Ge, S.-Y. Niu, Cryst. Growth Des. 9 (2009) 1525;
(e) Z. Wang, Y.-H. Xing, C.-G. Wang, L.-X. Sun, J. Zhang, M.-F. Ge, S.-Y. Niu, CrystEngComm 12 (2010) 762.

[5] (a) I. Rodrigues, I. Mihalcea, C. Volkringer, T. Loiseau, M. Visseaux, Inorg. Chem. 51 (1) (2012) 483;
(b) H. Zhu, P. Chen, C.-F. Yang, Y.-X. Wu, Macromol. React. Eng., doi: 10.1002/mren.201400063.

[6] S.G. Torres, Synthese neuer Carboxylate durch Oxidation von Metallen mit Liebig-Säuren (in German) (PhD thesis), Universität zu Köln, Germany, 2007

[7] (a) K. Binnemans, L. Jongen, C. Bromant, D. Hinz, G. Meyer, Inorg. Chem. 39 (2000) 5938;
(b) W.J. Evans, D.G. Giarikos, J.W. Ziller, Organometallics 20 (2001) 5751;
(c) M.A. Nabar, S.D. Barve, J. Appl. Crystallogr. 17 (1984) 39.

[8] (a) Y.-K. He, X.-F. Wang, L.-T. Zhang, Z.-B. Han, S. W. Ng, Acta Crystallogr., Sect. E: 63 (2007) m3019.;
(b) S.C. Manna, E. Zangrando, A. Bencini, C. Benelli, N.R. Chaudhuri, Inorg. Chem. 45 (2006) 9114;
(c) Q. He, J.-F. Zi, F.-J. Zhang, Acta Crystallogr., Sect. E 62 (2006) m1266.

[9] (a) C.-X. Wang, Z.-F. Li, P. Wang, Acta Crystallogr., Sect. C 63 (2007) m473;
(b) P. Zhu, W. Gu, M.-L. Liu, H.-B. Song, X. Liu, Y.-Q. Gao, H.-Y. Duan, S.-P. Yan, D.-Z. Liao, CrystEngComm 11 (2009) 351.

[10] R.D. Shannon, Acta Crystallogr. A 32 (1976) 751.

[11] (a) L.D. Almeida, S. Grandjean, N. Vigier, F. Patisson, Eur. J. Inorg. Chem. (2012) 4986;
(b) H. Hinode, R. Sharma, L. Eyring, J. Solid State Chem. 84 (1990) 102.

[12] (a) G. Socrates, Infrared and Raman Characteristic Group Frequencies: Tables and Charts, 3rd ed., John Wiley & Sons Hoboken, New York, 2004;
(b) R.L. Frost, Anal. Chim. Acta 517 (2004) 207;
(c) Y. Zhang, M. Bhadbhade, I. Karatchevtseva, J. Gao, J.R. Price, G.R. Lumpkin, Eur. J. Inorg. Chem. (2013) 6170;
(d) Y. Zhang, J.R. Price, I. Karatchevtseva, K. Lu, B. Yoon, F. Kadi, G.R. Lumpkin, F. Li, Polyhedron 91 (2015) 98;
(e) Y. Zhang, F. Kadi, I. Karatchevtseva, J.R. Price, T. Murphy, R. Wuhrer, F. Li, G.R. Lumpkin, J. Incl. Phenom. Macrocycl. Chem. 82 (1-2) (2015) 163;
(f) Y. Zhang, I. Karatchevtseva, F. Kadi, K. Lu, B. Yoon, J.R. Price, F. Li, G.R. Lumpkin, Polyhedron 87 (2015) 377;
(g) Y. Zhang, I. Karatchevtseva, J.R. Price, I. Aharonovich, F. Kadi, G.R. Lumpkin, Feng Li, RSC Adv. 5 (2015) 33249;
(h) Y. Zhang, M. Bhadbhade, J.R. Price, I. Karatchevtseva, N. Scales, L. Kong, G.R. Lumpkin, F. Li, Polyhedron 92 (2015) 99.

[13] (a) M. Suzuki, T. Shimanouchi, J. Mol. Spec. 20 (1968) 394;
(b) D.E. Morris, D.E. Hobart, J. Raman Spec. 19 (1988) 231;
(c) R.L. Frost, Anal. Chim. Acta 517 (1-2) (2004) 207.

[14] Bruker's APEX2, Bruker AXS Inc., Madison, Wisconsin, USA, 2007.

[15] T.M. McPhillips, S.E. McPhillips, H.J. Chiu, A.E. Cohen, A.M. Deacon, P.J. Ellis, E. Garman, A. Gonzalez, N.K. Sauter, R.P. Phizackerley, S.M. Soltis, P. Kuhn, J. Synchrotron Rad. 9 (2002) 401.

[16] W. Kabsch, Appl. Crystallogr. 26 (1993) 795.

[17] G.M. Sheldrick, Acta Crystallogr. A64 (2008) 112.

[18] O.V. Dolomanov, L.J. Bourhis, R.J. Gildea, J.A.K. Howard, H. Puschmann, J. Appl. Crystallogr. 42 (2009) 339.

[19] A.L. Spek, Acta Crystallogr. D65 (2009) 148.